CHEMISTRY
A EUROPEAN JOURNAL

DOI: 10.1002/chem.200902944

DABCO-Mediated Self-Assembly of Zinc Porphyrin–Perylene Bisimide Monodisperse Multichromophoric Nanoparticles**

Peter Osswald, Chang-Cheng You, Vladimir Stepanenko, and Frank Würthner*[a]

Dedicated to Professor Arndt Simon on the occasion of his 70th birthday

The light-harvesting systems (LHS) of photosynthetic plants and bacteria have inspired the design of a multitude of artificial dye assemblies to mimic the functional properties of natural LHS. The primary focus of most of those studies was on the incorporation of a multitude of dyes in a defined molecular framework and the elucidation of energy-transfer efficiencies between the constituent dyes. The dendrimer concept has been shown to be very successful in this regard and molecular systems incorporating up to 32 dye units have been achieved.[1]

Metalloporphyrins and perylene bisimides (PBIs) are amongst the most frequently applied chromophores for artificial dye assemblies. While in natural LHS the protein matrix controls the position and orientation of the dye manifold in a rather precise manner, most artificial constructs, however, have to be considered as conformationally ill-defined with more or less randomly oriented and fluctuating transition dipole moments.

Herein, we introduce a small model system composed of four metalloporphyrins that are tethered to a PBI dye core by quite a long spacer unit, respectively. Our spectroscopic and microscopic studies reveal that this conformationally ill-defined pentachromophoric system can be transformed to a well-defined three-dimensional nanoobject by noncovalent binding of a small-molecule additive that, in a sense, mimics the role of the protein matrix. Our approach is based on the well-established interaction of zinc porphyrins and the ditopic 1,4-diazabicyclo[2.2.2]octane (DABCO) ligand, which exhibits high binding constants.[2]

Thus, we have synthesized the tetra(zinc porphyrin)-functionalized PBI building block **4** according to the route depicted in Scheme 1. The esterification of tetra(3-hydroxyphenoxy) PBI **1** with free-base porphyrin carboxylic acid **2** (for the synthesis of **1** and **2**, see the Supporting Information) using dicyclohexylcarbodiimide (DCC) and 4-(*N*-dimethylamino)pyridinium toluene sulfonate (DPTS) as coupling reagents in dichloromethane at room temperature provided the free-base porphyrin–PBI conjugate **3** in 33% yield. Subsequent metallation of **3** in dichloromethane with a saturated solution of zinc acetate in methanol afforded the target pentachromophoric system **4** in pure form after silica-gel column chromatography with chloroform as eluent in 57% yield. Compound **4** was properly characterized by ^{1}H NMR spectroscopy, MALDI-TOF mass spectrometry, and elemental analysis (for details, see the Supporting Information).

The optical properties of **4** were investigated by UV/Vis spectroscopy in chloroform. The absorption spectrum of **4** is dominated by the intense Soret band of the zinc porphyrin (420–430 nm), whereas in the Q-band region of the porphyrin (500–650 nm) the absorptions of both chromophores overlap (Figure 1). A comparison of the UV/Vis spectrum of **4** with that of the parent zinc tetraphenylporphyrin (ZnTPP)[3] reveals a good agreement for the Soret band (423 nm), indicating that no ground-state interaction between the zinc porphyrin units and the PBI of **4** is present. By contrast, in the Q-band region significant spectral differences are observed that can be attributed to the PBI chromophore. The difference spectrum (see Figure 1, inset) of **4** and four ZnTPP moieties (the spectrum of ZnTPP is magnified by a factor of four, since **4** contains four ZnTPP unites) shows the characteristic spectral features of aryloxy-substituted PBIs with an absorption maximum at 569 nm, which is in good agreement with the values reported for such PBIs.[4] Accordingly, the longest wavelength transition in the absorption spectrum of **4** (Figure 1, inset) can be attributed to

[a] Dr. P. Osswald, Dr. C.-C. You, Dr. V. Stepanenko, Prof. Dr. F. Würthner
Universität Würzburg, Institut für Organische Chemie and Röntgen Research Center for Complex Material Systems
Am Hubland, 97074 Würzburg (Germany)
Fax: (+49) 931-31-84756
E-mail: wuerthner@chemie.uni-wuerzburg.de

[**] DABCO = 1,4-diazabicyclo[2.2.2]octane

Supporting information for this article is available on the WWW under http://dx.doi.org/10.1002/chem.200902944.

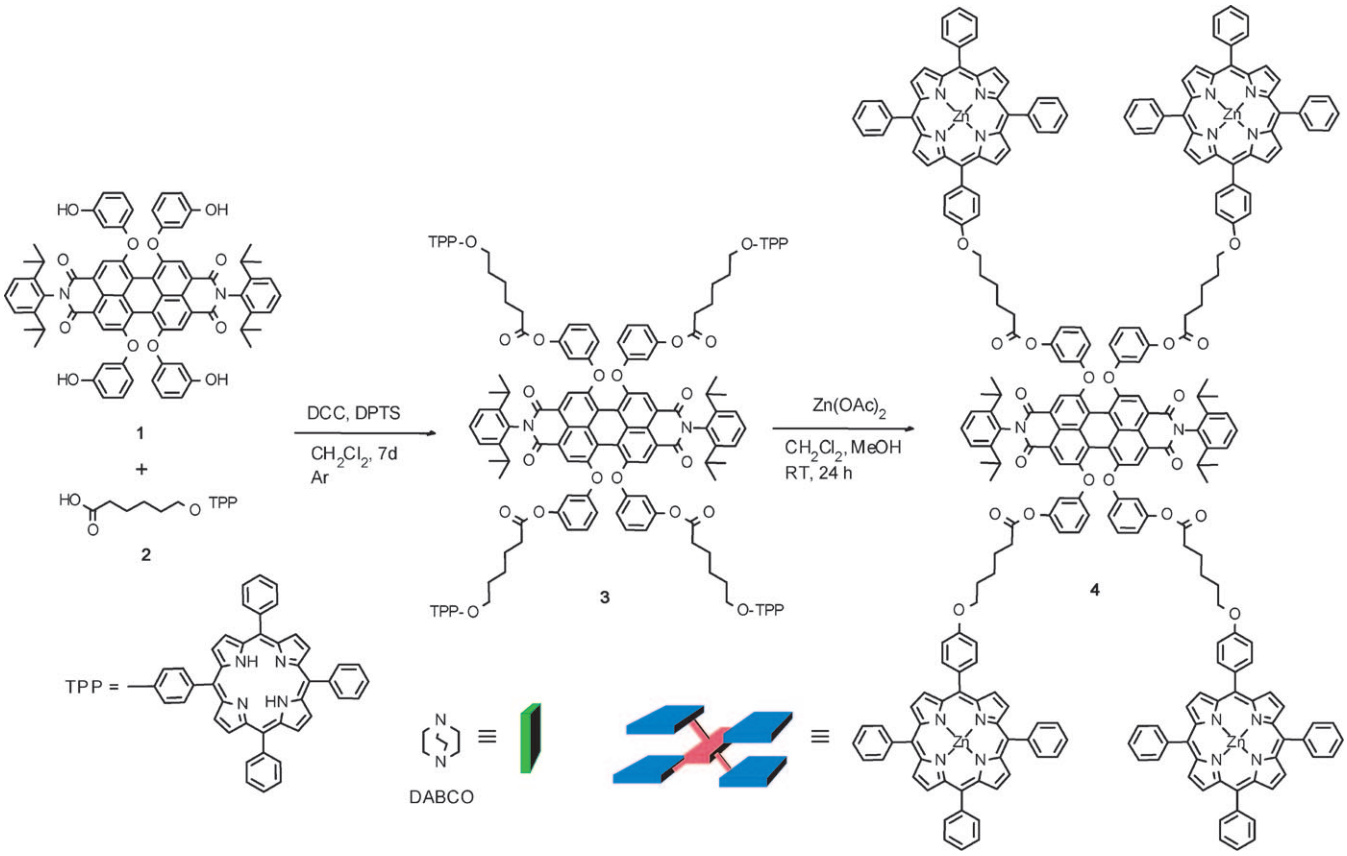

Scheme 1. Synthesis of tetra(zinc porphyrin)-functionalized PBI **4** and schematic representation of **4** and DABCO.

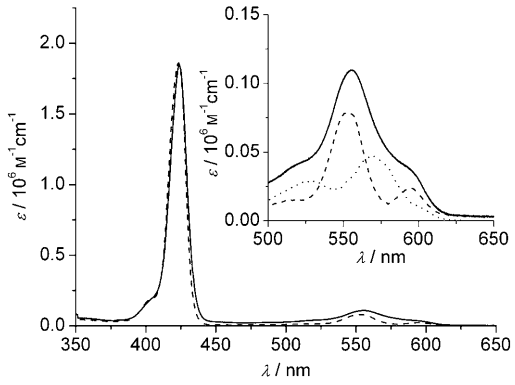

Figure 1. Comparison of the absorption spectra of **4** (solid line) and ZnTPP (magnified by a factor of four, dashed line) in chloroform. Inset: An expansion of the Q-band region of absorption spectra of **4** (solid line) and ZnTPP (dashed line), and difference spectrum of **4** and ZnTPP (dotted line) in chloroform.

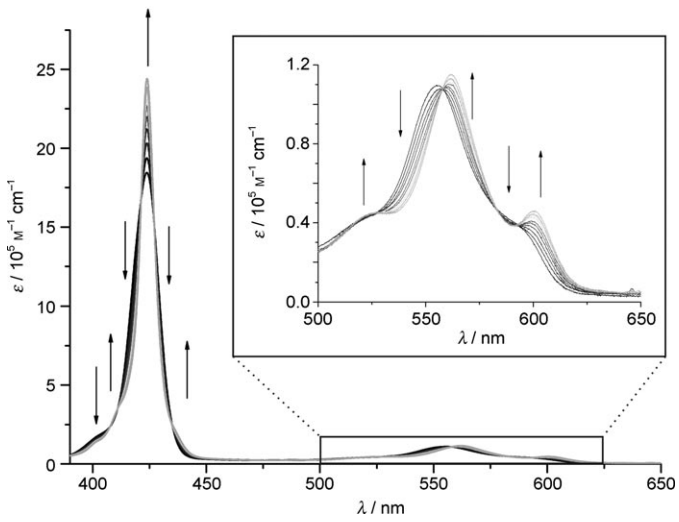

Figure 2. UV/Vis titration of **4** ($c = 9 \times 10^{-7}$ M) with DABCO in $CHCl_3$ at 23 °C. Inset: an expansion of the Q-band region. Arrows indicate spectral changes with increasing amounts of DABCO (from 0 to 2 molar ratio).

both chromophores (ZnTPP, PBI), which exhibit almost equal $S_0 \rightarrow S_1$ excitation energy.[3]

The self-assembly of **4** with DABCO was investigated by constant host titration by using UV/Vis spectroscopy. Figure 2 shows the absorption spectra of **4** in chloroform upon successive addition of DABCO. During the titration, a distinct band arises at 601 nm and the broad Soret band gets narrowed with a concomitant increase in intensity as the half-width of the Soret band changes from 770 to 436 cm^{-1}. The appearance of a clearly recognizable absorption band at 601 nm upon ligation of DABCO with the zinc porphyrin units readjusts the energy levels in such a way that the lowest excited state can now be clearly attributed to the

ZnTPP units. The position of the Soret band at 424 nm, as previously observed for ZnTPP–DABCO sandwich complexes,[2g] supports the formation of a sandwich complex.[5] The spectral changes observed upon ligation of DABCO to the multichromophoric building block **4** apparently stem from a more defined arrangement of the chromophore units that restricts the conformational flexibility of the system.

During the titration, isosbestic points (at 421, 427, 435, 557, 579, 592 nm) were observed up to a 1:1 ratio of **4** and DABCO, implying that two species are present in equilibrium. Upon further addition of DABCO up to a ratio of 1:2 (**4**/DABCO), a second process emerges that is characterized by slightly displaced isosbestic points (421, 427, 434, 558, 582, 591 nm). These observations imply that two individual two-state equilibria are involved in this self-assembly process. A schematic representation of the possible equilibria is shown in Figure 3. The titration data were analyzed by non-

Figure 3. Schematic representation of a two-step formation of self-assembled macrocycles and definition of the respective binding constants. The PBI is shown in red, the zinc porphyrin in blue, and DABCO ligand in green.

linear least-squares analysis[6] by using a model consisting of 1:0, 1:1, and 1:2 species (see Figure S4 in the Supporting Information). The binding constant for the formation of the 1:1 species, K_{11}, was determined to be $(1.3\pm0.3)\times10^{7}\,\text{M}^{-1}$ and for the equilibrium between the 1:1 and the 1:2 species (K_{12}) a value of $(5.6\pm1.5)\times10^{6}\,\text{M}^{-1}$ was obtained.

The UV/Vis titration experiments described above reveal a stepwise ligation of DABCO at the zinc coordination site. In principle, self-assembly of multifunctional compounds can lead to the formation of polymeric entities or defined macrocycles. The comparison of the binding constants estimated for the DABCO-mediated self-assembly of **4** with those of previously reported systems leading to macrocyclic structures,[2k] however, strongly suggests the formation of two macrocyclic structures in a "figure-eight"-type arrangement, as schematically shown in Figure 3. Accordingly, well-positioned transition dipole moments are evoked by DABCO coordination, while more or less random orientation of the transition dipole moments of the five chromophore units prevails in the precursor molecule **4**.

Subsequently, a ^{1}H NMR spectroscopic titration was carried out in deuterated chloroform at 300 K under constant host conditions with a 0.67 mM solution of **4**. Upon successive addition of DABCO (0 to 2 equiv) to a solution of **4** in chloroform, the signals of β-pyrrole protons of porphyrin at $\delta=8.8$ ppm (center of multiplet) decreased gradually and a new resonance arose at around $\delta=8.5$ ppm (Figure 4).[7] At a 1:2 ratio of **4** and DABCO, the initial signal at $\delta=8.8$ ppm disappeared completely and the newly emerged signal at $\delta=$

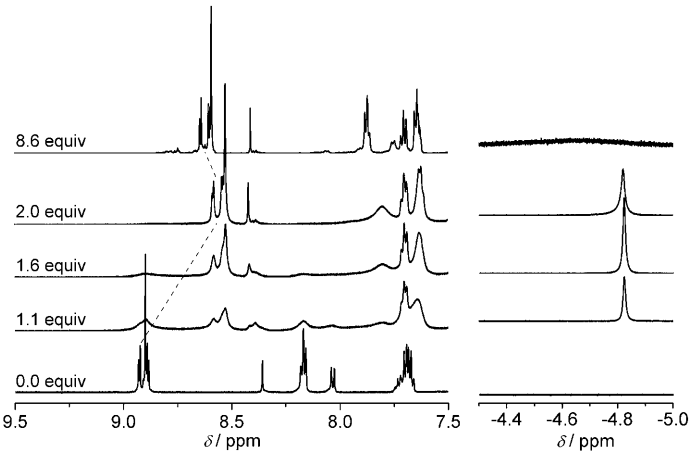

Figure 4. Sections of the ^{1}H NMR spectra (600 MHz) of **4** (6.4×10^{-4} M) recorded during the titration with DABCO in $CDCl_3$. Aromatic resonances (left) and the high-field region (right) with DABCO resonances are depicted. The number of equivalents of DABCO added is indicated on each spectrum.

8.5 ppm sustained with higher intensity. This observation supports the 1:2 stoichiometry of the complex formed, and thus corroborates the results of UV/Vis titration experiments. The characteristic upfield shift of porphyrin resonances (0.3 ppm) indicates the formation of a double-decker structure in which the aromatic ring current of the two porphyrins influence each other. This is further confirmed by the very pronounced upfield shift of DABCO methylene protons ($\delta=-4.8$ ppm), since this is a typical ^{1}H NMR spectroscopy signature for zinc porphyrin–DABCO sandwich complexes.[2g] At a 1:2 stoichiometry of **4** and DABCO, the PBI and zinc porphyrin resonances are well resolved and appear sharp, indicating the formation of a structurally well-defined assembly, namely, 1:2 (**4**/DABCO) complex, rather than polymeric species. Upon the addition of more than two equivalents of DABCO, the corresponding DABCO signal gets broadened and shifted downfield, and almost disappeared at a ratio of 8:1 (DABCO/**4**). Such behavior was often observed in similar systems and attributed to an exchange process of the bound and free DABCO molecules on the NMR timescale.[2g]

To provide further evidence that no polymers or higher cyclic oligomers are created by self-assembly of **4** and DABCO, two-dimensional DOSY NMR spectroscopy experiments were performed in $CDCl_3$. The DOSY spectra were recorded first for the host **4** and then after the addition of two equivalents of DABCO for the complex **4**·$(DABCO)_2$. The diffusion coefficients were determined as the mean value of ten individual signals. The obtained values for the free host **4** ($2.29\times10^{-10}\,\text{m}^2\,\text{s}^{-1}$) and a 1:2 (**4**/DABCO) sample ($2.33\times10^{-10}\,\text{m}^2\,\text{s}^{-1}$) do not differ significantly, revealing that the species formed by self-assembly of **4** with DABCO at a 1:2 ratio should be of similar size as **4**, which is actually in compliance with the fact that the molecular weights of **4** and 1:2 (**4**/DABCO) complex do not differ substantially. From the diffusion coefficients, the hydrody-

namic radii of the molecules can be calculated by employing the Stokes–Einstein Equation (1) under the assumption of spherical particles:[8]

$$D = \frac{k_B T}{6\pi\eta r} \quad (1)$$

According to Equation (1), radii of 1.59 and 1.56 nm were estimated for **4** and **4**·$(DABCO)_2$ complex, respectively. Pleasingly, this value (1.56 nm) for the **4**·$(DABCO)_2$ complex is in excellent agreement with the radius (1.54 nm) obtained from molecular modeling (Figure 5 and Figure S2 in the Supporting Information). These results confirm that no polymers are formed by the self-assembly of **4** and DABCO, rather discrete structures are created at a 1:2 (**4**/DABCO) stoichiometry.[9]

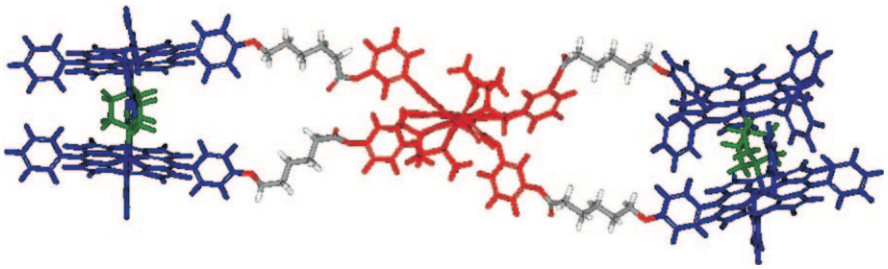

Figure 5. Structure of **4**·$(DABCO)_2$ obtained from molecular modeling. A laterally (stretched conformation) bridged structure was calculated with a MM3 force field by using a CaChe Quantum CaChe Workspace 5.0. View is along the *N*,*N*-axis of the PBI. The PBI is highlighted in red, zinc porphyrins in blue, and DABCO in green.

In principle, two isomers are possible for the macrocyclic structure of **4**·$(DABCO)_2$, since upon complexation the DABCO molecules can link two zinc porphyrins either in a lateral or a diagonal manner (as shown in Figure 5 and Figure S2 in the Supporting Information).[10,11] Unfortunately, in contrast to structurally similar covalent macrocycles,[10] the two possible isomers of the present supramolecular macrocycle cannot be distinguished by spectroscopic means. However, since aryloxy-substituted PBIs prefer a horizontal orientation of the aryloxy residues,[10] and the building block **4** contains such residues, the laterally bridged isomer (Figure 5) should be more probable structure for the self-assembled macrocycle **4**·$(DABCO)_2$.

To assess the self-organization behavior of **4**·$(DABCO)_2$ on surfaces, AFM analysis was performed on highly ordered pyrolytic graphite (HOPG) in tapping mode. In AFM images of self-assembled **4**·$(DABCO)_2$ macrocycles (Figure 6 B–D), a highly ordered pattern was observed over a wide range of the surface. For comparison, a sample of uncomplexed building block **4** was analyzed under similar conditions (Figure 6 A). In contrast to **4**·$(DABCO)_2$, compound **4** showed only ill-defined agglomerates on the surface, indicating that the defined arrangement of the chromophores in **4**·$(DABCO)_2$ complexes is responsible for the observed unique ordering of these complexes on the surface. High-resolution AFM images of **4**·$(DABCO)_2$ (Figure 6 C, D) clearly show small isolated nanosized particles that are arranged in distorted hexagonal packing on the surface. It is noteworthy that, in contrast to DABCO, the more extended 4,4′-dipyridine ligand as an additive did not afford any well-defined structures (see AFM images in Figure S3 in the Supporting Information). This implies that a proper size of the additive is decisive for the formation of well-defined nanoobjects of the present multichromophoric system.

For the observed ellipsoid particles of **4**·$(DABCO)_2$, an average length of (4.7 ± 0.5) nm and width of (3.4 ± 0.5) nm were determined by Fourier transformation. The height of the particles was elucidated by cross-section analysis as 0.48 nm, indicating the presence of a monolayer. Based on these data, the area covered by each supramolecular particle was estimated to be 12.6 nm^2. Again, the particle size determined by AFM analysis fits well with the dimensions (10.9 nm^2) of the macrocyclic structure calculated by molecular modeling, confirming the monodisperse nature of the particles. These results clearly demonstrate that the well-defined self-assembled macrocycles **4**·$(DABCO)_2$ can be deposited on surfaces by spin-coating as single molecular entities in a highly ordered pattern.

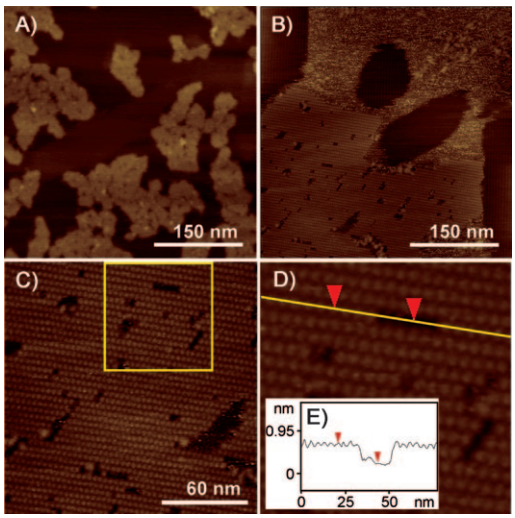

Figure 6. Height AFM images of a 1×10^{-5} M solution of **4** (A) and **4**·$(DABCO)_2$ (B–D) in chloroform spin-coated on HOPG under 5000 rpm, and cross-section analysis (E, along the yellow line in D). Image D is a magnified region of image C (yellow frame). The scale bars are 150 (A, B) and 60 nm (C), and the *z* scale is 2 nm.

In summary, a novel multichromophoric system **4** based on zinc porphyrin and PBI dyes was synthesized. Taking to-

gether all the results of the present spectroscopic and microscopic investigations, it can be concluded that the DABCO-mediated self-assembly of **4** occurred with high binding constants under exclusive formation of a singular species with well-positioned dipole moments. The self-assembled **4**·$(DABCO)_2$ macrocycles can be deposited on a graphite surface by spin-coating to afford a regular 2D adlayer of photofunctional monodisperse nanoparticles. Such multichromophoric nanoobjects incorporating well-oriented chromophore units are still rare in supramolecular chemistry, although they are ubiquitously present in natural light-harvesting protein complexes[12] that likewise organize to intriguing 2D patterns in photosynthetic membranes.[13] The defined arrangement of the chromophores and the highly ordered structure of the present multichromophoric nanoparticles on surfaces may lead to applications as electro- or photoactive materials where such particles can be addressed individually.[14]

Experimental Section

For experimental details, see the Supporting Information.

Acknowledgements

We thank the Alexander von Humboldt Foundation for a postdoctoral fellowship (C.C.Y.) and the DFG for financial support (grant project: WU 317/7).

Keywords: dyes/pigments · multichromophore systems · porphyrinoids · scanning probe microscopy · self-assembly

[1] For recent reviews, see: a) V. Balzani, G. Bergamini, P. Ceroni, F. Vögtle, *Coord. Chem. Rev.* **2007**, *251*, 525–535; b) A. C. Grimsdale, K. Müllen, *Angew. Chem.* **2005**, *117*, 5732–5772; *Angew. Chem. Int. Ed.* **2005**, *44*, 5592–5629; c) S. Hecht, J. M. J. Fréchet, *Angew. Chem.* **2001**, *113*, 76–94; *Angew. Chem. Int. Ed.* **2001**, *40*, 74–91.

[2] a) H. L. Anderson, C. A. Hunter, M. N. Meah, J. K. M. Sanders, *J. Am. Chem. Soc.* **1990**, *112*, 5780–5789; b) C. A. Hunter, M. N. Meah, J. K. M. Sanders, *J. Am. Chem. Soc.* **1990**, *112*, 5773–5780; c) C. C. Mak, N. Bampos, J. K. M. Sanders, *Angew. Chem.* **1998**, *110*, 3169–3172; *Angew. Chem. Int. Ed.* **1998**, *37*, 3020–3023; d) C. C. Mak, D. Pomeranc, M. Montalti, L. Prodi, J. K. M. Sanders, *Chem. Commun.* **1999**, 1083–1084; e) P. N. Taylor, H. L. Anderson, *J. Am. Chem. Soc.* **1999**, *121*, 11538–11545; f) C. C. Mak, N. Bampos, S. L. Darling, M. Montalti, L. Prodi, J. K. M. Sanders, *J. Org. Chem.* **2001**, *66*, 4476–4486; g) L. Baldini, P. Ballester, A. Casnati, R. M. Gomila, C. A. Hunter, F. Sansone, R. Ungaro, *J. Am. Chem. Soc.* **2003**, *125*, 14181–14189; h) T. Hirao, K. Saito, *Macromol. Symp.* **2003**, *204*, 103–112; i) M. C. Lensen, S. J. T. van Dingenen, J. A. A. W. Elemans, H. P. Dijkstra, G. P. M. van Klink, G. van Koten, J. W. Gerritsen, S. Speller, R. J. M. Nolte, A. E. Rowan, *Chem. Commun.* **2004**, 762–763; j) D. I. Schuster, K. Li, D. M. Guldi, J. Ramey, *Org. Lett.* **2004**, *6*, 1919–1922; k) P. Ballester, A. Costa, A. M. Castilla, P. M. Deyà, A. Frontera, R. M. Gomila, C. A. Hunter, *Chem. Eur. J.* **2005**, *11*, 2196–2206; l) P. B. Ballester, A. I. Oliva, P. M. Deyà, A. Frontera, R. M. Gumila, C. A. Hunter, *J. Am. Chem. Soc.* **2006**, *128*, 5560–5569; m) L. Flamigni, B. Ventura, A. I. Oliva, P. Ballester, *Chem. Eur. J.* **2008**, *14*, 4214–4224; n) T. Kishida, N. Fujita, O. Hirata, S. Shinkai, *Org. Biomol. Chem.* **2006**, *4*, 1902–1909; o) T. Ishida, Y. Morisaki, Y. Chujo, *Tetrahedron Lett.* **2006**, *47*, 5265–5268.

[3] a) F. D'Souza, S. Gadde, M. E. Zandler, K. Arkady, M. E. El-Khouly, M. Fujitsuka, O. Ito, *J. Phys. Chem. A* **2002**, *106*, 12393–12404; b) C.-C. You, R. Dobrawa, C. R. Saha-Möller, F. Würthner, *Top. Curr. Chem.* **2005**, *258*, 39–82; c) M. Ghirotti, C. Chiorboli, C.-C. You, F. Würthner, F. Scandola, *J. Phys. Chem. A* **2008**, *112*, 3376–3385.

[4] E. Fron, G. Schweitzer, P. Osswald, F. Würthner, P. Marsal, D. Beljonne, K. Müllen, F. C. De Schryver, M. van der Auweraer, *Photochem. Photobiol. Sci.* **2008**, *7*, 1509–1521.

[5] Note that a redshift of 5 nm (from 420 to 425 nm) was previously taken as evidence for the formation of a sandwich complex. This redshift was not observed in the present case, possibly due to the presence of slight amounts of water or ethanol (stabilizer of chloroform), the coordination of which to the metalloporphyrin causes similar spectral shifts; see also: a) S. Yagi, M. Ezoe, I. Yonekura, T. Takagishi, H. Nakazumi, *J. Am. Chem. Soc.* **2003**, *125*, 4068–4069; b) W.-S. Li, D.-L. Liang, Y. Suna, T. Aida, *J. Am. Chem. Soc.* **2005**, *127*, 7700–7702.

[6] SpecFit/32 from Spectrum Software Associates (Marlborough, MA, 2000–2001) was used for data analysis.

[7] The slight broadening of the signals stems from an intramolecular dynamic process evoked by the increased barrier for the inversion process between the (*P*)- and (*M*)-atropoenantiomers (see P. Osswald, F. Würthner, *J. Am. Chem. Soc.* **2007**, *129*, 14319–14326) of the core-tetrasubstituted PBI as the temperature-dependent spectra of **4**·$(DABCO)_2$ reveal (Figure S1 in the Supporting Information). Upon cooling from 293 to 273 K, a significant sharpening of the signals was observed, especially of those related to the aryloxy residues attached to the perylene core. Whereas the signal for DABCO protons remained unchanged, indicating that complexation is not influenced by temperature change.

[8] a) H. J. V. Tyrrell, K. R. Harris, *Diffusion in Liquids: A Theoretical and Experimental Study*, Butterworths, London, **1984**.

[9] Unfortunately, all attempts to record mass spectra for the complex **4**·$(DABCO)_2$ by ESI-TOF MS or MALDI-TOF MS failed. Only the molecular ion of **4** could be observed. This is very often the case for self-assembled systems and is attributed to the reversible nature of the self-assemblies and the lability of such self-assembled systems under the conditions of ionization (also see C. M. Drain, I. Goldberg, I. Sylvain, A. Falber, *Top. Curr. Chem.* **2005**, *245*, 55–88).

[10] a) P. Osswald, D. Leusser, D. Stalke, F. Würthner, *Angew. Chem.* **2005**, *117*, 254–257; *Angew. Chem. Int. Ed.* **2005**, *44*, 250–253; b) P. Osswald, F. Würthner, *Chem. Eur. J.* **2007**, *13*, 7395–7409.

[11] Two additional isomeric macrocycles are possible by 1,6- and 7,12-linkage. In contrast to the lateral and diagonal isomer (D_2), these two isomers exhibit less symmetry as they belong to the symmetry group C_2. Therefore, these isomers can be excluded due to the observed symmetrical NMR spectroscopy pattern of the self-assemblies. This is further supported by the fact that these two straight bridged isomers are energetically less favored.

[12] a) T. Pullerits, V. Sundström, *Acc. Chem. Res.* **1996**, *29*, 381–389; b) T. S. Balaban, H. Tamiaki, A. R. Holzwarth, *Top. Curr. Chem.* **2005**, *258*, 1–38; c) T. Brixner, J. Stenger, H. M. Vaswani, M. Cho, R. E. Blankenship, G. R. Fleming, *Nature* **2005**, *434*, 625–628.

[13] S. Scheuring, J. N. Sturgis, V. Prima, A. Bernadac, D. Lévy, J.-L. Rigaud, *Proc. Natl. Acad. Sci. USA* **2004**, *101*, 11293–11297.

[14] H. Uji-i, A. Miura, A. P. H. Schenning, E. W. Meijer, Z. Chen, F. Würthner, F. C. De Schryver, M. van der Auweraer, S. De Feyter, *ChemPhysChem* **2005**, *6*, 2389–2395.

Received: October 23, 2009
Published online: January 28, 2010

